Enhanced conductivity of tunnel junctions employing semimetallic nanoparticles through variation in growth temperature and deposition

Hari P. Nair,[a] Adam M. Crook, and Seth R. Bank
Microelectronics Research Center, University of Texas at Austin, 10100 Burnet Rd., Austin, Texas 78758, USA

(Received 29 March 2010; accepted 4 May 2010; published online 1 June 2010)

We report ErAs nanoparticle-enhanced tunnel junctions grown on GaAs with low specific resistances ($<2\times10^{-4}$ Ω cm^{-2}), approximately tenfold lower than previous reports. A reduction in specific resistance was achieved by modifying the ErAs nanoparticle morphology through the molecular beam epitaxial growth conditions, particularly lower growth temperatures. A further investigation of the variation in tunnel junction resistance with the amount of ErAs deposited and growth temperature shows that nanoparticle surface coverage may not be the only factor determining tunnel junction resistance. *© 2010 American Institute of Physics.*
[doi:10.1063/1.3442909]

Tunnel junctions are essential for enhancing the performance of many important photonic devices. Tunnel junctions are used to interconnect the different band gap junctions in multijunction tandem solar cells.[1] They are also used in vertical-cavity surface-emitting lasers (VCSELs), to reduce p-type free carrier absorption[2] and series resistance associated with the p-type DBR, by replacing it with a n-type DBR and a tunnel junction.[3] An ideal tunnel junction for these applications should be capable of conducting high current densities (>1 kA/cm^2 for VCSELs), with simultaneously low electrical and optical losses. Here we demonstrate tunnel junctions enhanced with semimetallic nanoparticles that achieve low specific resistances with relatively low doping densities. This is advantageous as it mitigates dopant diffusion effects during post-growth thermal processes and reduces free carrier absorption losses, such as in long-wavelength semiconductors lasers.

As shown in Fig. 1(a), a conventional tunnel junction consists of a heavily doped p^+/n^+ junction, where band-to-band tunneling between the valence band and the conduction band is the dominant current flow mechanism. The tunneling current density increases exponentially with decreasing band gap (tunneling barrier height) and depletion layer thickness (tunneling distance). However, reducing the band gap of the tunnel junction leads to increased optical absorption in the device. In a multijunction solar cell, electron–hole pairs generated from optical absorption in the tunnel junction do not contribute to the cell current, reducing the power conversion efficiency of the cell.[4] Since reducing the band gap of the tunnel junction is often not a viable option, a variety of other techniques have been used to reduce the tunneling resistance. One approach is to decrease the tunneling distance by increasing the doping in the tunnel junction. For a GaAs-based tunnel junction, this poses some fundamental difficulties, such as compensation of donors if silicon is used as the n-type dopant, limiting the maximum achievable doping concentration to $\sim5\times10^{18}$ cm^{-3}. Although this limit can be overcome by growing at low temperatures to achieve higher doping concentrations,[5] the resulting tunnel junctions degrade when subjected to post growth rapid thermal annealing. Another option is to use donors, such as tellurium, which can achieve marginally higher active dopant concentrations. However, this leads to further issues including memory effect and decreasing incorporation efficiency at higher growth temperatures, due to the high vapor pressure of tellurium.[6] Yet another approach for fabricating tunnel junctions is to exploit a type-II band alignment,[7] where the effective barrier height for tunneling is reduced. This approach is limited by

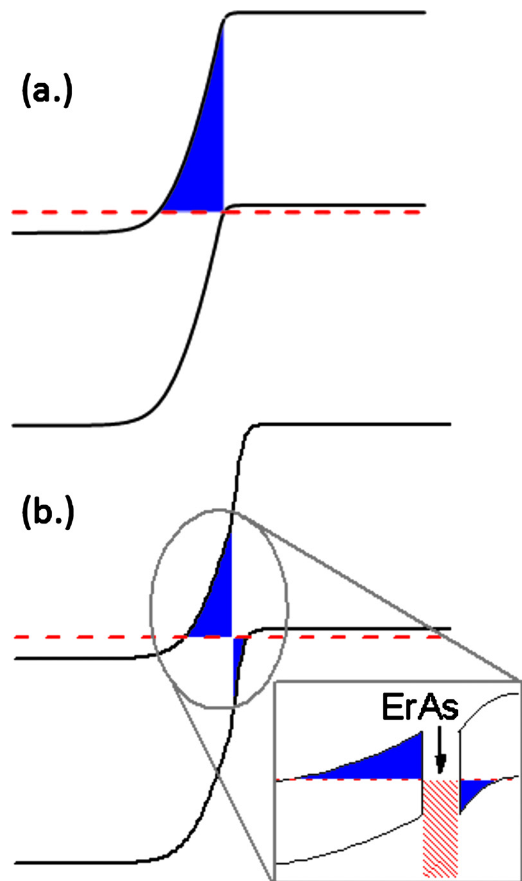

FIG. 1. (Color online) Band diagram of (a) a conventional tunnel junction and (b) an ErAs nanoparticle-enhanced tunnel junction illustrating the back-to-back Schottky contacts. The shaded regions represent the tunneling barrier for electrons.

[a]Electronic mail: hnair@mail.utexas.edu.

 © 2010 American Institute of Physics

Author complimentary copy. Redistribution subject to AIP license or copyright, see http://apl.aip.org/apl/copyright.jsp

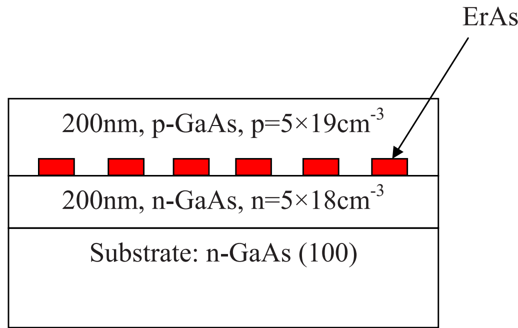

FIG. 2. (Color online) Layer structure of the ErAs nanoparticle-enhanced tunnel junctions.

the amount of strain that can be accommodated in the tunnel junction, without introducing dislocations, and also to only a few fortuitous materials systems, such as $In_{0.52}Al_{0.48}As/InP$.

Incorporation of semimetallic ErAs nanoparticles at the p^+/n^+ interface of a conventional GaAs tunnel junction leads to a significant improvement in tunneling current density. According to Pohl *et al.*,[8] as illustrated in Fig. 1(b), the enhancement can be understood by visualizing the incorporation of ErAs nanoparticles at the interface as forming two back-to-back Schottky contacts with the Fermi level pinned at approximately the middle of the band gap. In this arrangement, the single band-to-band tunneling step is divided into two shorter tunneling steps, each of only half the barrier height and half the tunneling distance. Since the tunneling probability increases exponentially with either term, the current density through the diode increases by >five orders of magnitude.[8] Since the tunneling takes place into a continuum of states in the band gap, these tunnel junctions do not exhibit an Esaki peak in forward bias.[8] Zide *et al.*,[9] has demonstrated a twofold improvement in efficiency of a dual-junction tandem solar cell using ErAs nanoparticle-enhanced tunnel junctions to interconnect the junctions. Here we investigate the performance trends in ErAs nanoparticle enhanced tunnel junctions with respect to (1) the amount of ErAs deposited at the interface and (2) the growth temperature.

ErAs is a rocksalt semimetal[10] with a 1.6% lattice mismatch to GaAs. It self-assembles in an islanding growth mode (Volmer–Weber) on a GaAs surface. The islands grow to an average thickness/width of three to four monolayers (ML) and then grow laterally outward to form a complete film.[11] This minimum height of 3–4 ML is required to stabilize a unit cell of the ErAs rocksalt crystal structure.[12] The lateral extent of the islands is determined by the erbium adatom surface diffusion length. Overgrowth of a complete ErAs layer with GaAs is difficult due to the formation of antiphase domains, because of the fourfold rotational symmetry of the ErAs rocksalt structure when compared to the twofold rotational symmetry of the GaAs zincblende structure.[13] However, if a complete ErAs film is not formed, then the exposed GaAs can seed the overgrowth of the ErAs nanoparticles, without forming antiphase domains.[13] Since it takes 3–4 ML of effective ErAs deposition to form a complete film, overgrowth can be achieved by keeping the amount of ErAs deposited well below 3–4 ML.[11]

ErAs nanoparticle-enhanced tunnel junctions were grown in a Varian Gen. II solid-source molecular beam epitaxy system equipped with a valved cracker for arsenic, a Veeco SUMO effusion cell for gallium, and a high-temperature effusion cell for erbium. The growths were carried out on silicon-doped (100) GaAs wafers with an electron concentration of $1-5\times10^{18}$ cm^{-3}. The layer structure is sketched in Fig. 2. The growth temperature was 530 °C, as measured by an optical pyrometer that was calibrated to the GaAs surface oxide desorption temperature. The As_2/Ga beam equivalent pressure (BEP) ratio was 20, while the As_2/Er BEP ratio was 121. A set of three samples were grown where the amount of ErAs deposited was varied, while keeping all other parameters fixed. Post growth, the samples were processed into mesa contact structures. Circular top Ohmic contacts were evaporated using Pd/Ge/Ti/Pt/Au. The back side Ohmic contact was formed using evaporated Pd/Ti/Pd/Au on the entire back of the sample. Devices were annealed in forming gas for 1 min at 450 °C. The remainder of the p-GaAs contact layer was removed after metallization using citric acid:H_2O_2:H_2O. The tunnel junction resistance was extracted by the method in Denhoff.[14] Parasitic resistances accounted for <1.5% of the overall measured resistance.

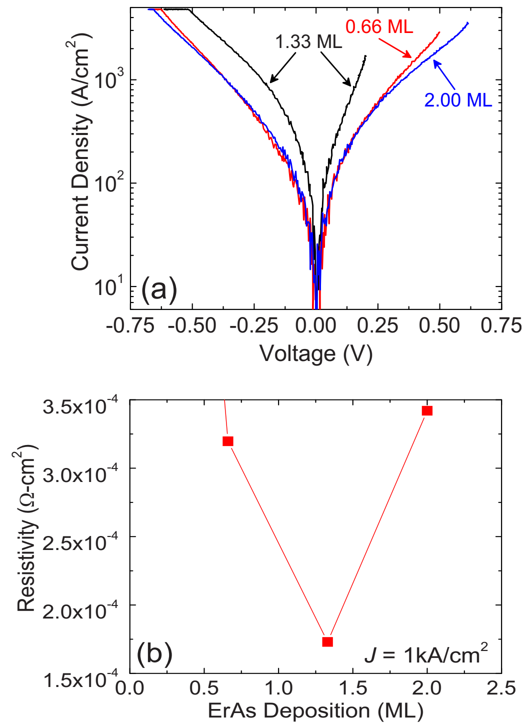

FIG. 3. (Color online) (a) Tunnel junction current density vs voltage and (b) tunnel junction resistivity variation with ErAs deposition. Note the absence of Esaki peak in forward bias. The resistance of the tunnel junction decreased initially as the amount of ErAs deposited was increased and then increased again at elevated depositions, showing a competition between surface coverage and morphology of the ErAs islands.

A growth temperature of 530 °C, 70 °C lower than that reported by Pohl *et al.*,[8] yielded the lowest resistance tunnel junctions. The sample with 1.33 ML of ErAs grown at 530 °C has a specific resistance of 1.73×10^{-4} $\Omega\ cm^2$, while the sample reported in Pohl *et al.*[8] and Zide *et al.*[9] reported a specific resistance of 1×10^{-3} $\Omega\ cm^2$. This further enhancement is most likely due to the lower growth temperature, because the doping densities and amount of ErAs (number of ML) between the two samples are comparable.

An important trend in the tunnel junction resistance occurred by varying the amount of ErAs deposited. As the deposition of ErAs increased, the surface coverage of ErAs

Author complimentary copy. Redistribution subject to AIP license or copyright, see http://apl.aip.org/apl/copyright.jsp

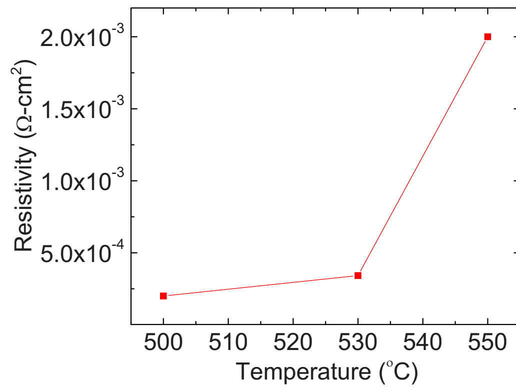

FIG. 4. (Color online) Resistivity of tunnel junctions containing 2 ML of ErAs vs growth temperature. Resistance increased at elevated growth temperatures, potentially due to increasing ErAs nanoparticle size.

nanoparticles also increased. One might expect the tunnel junction resistance to decrease monotonically with increasing ErAs deposition, based upon interfacial area considerations. Instead, the tunnel junction resistance (Fig. 3) initially decreased and then increased at elevated deposition. This suggests that surface coverage is not the only factor that determines the tunnel junction resistance. A probable explanation for this trend could be a competition between surface coverage and size of ErAs nanoparticles. As the amount of ErAs deposited increases, the nanoparticles ripen into larger particles.[11] We propose that the electrical resistance for tunneling into larger nanoparticles is greater than that into smaller particles. This may be associated with the difficulty in overgrowing larger nanoparticles.[11,15] Another possible explanation for this behavior could be due to a morphological dependence of the Schottky barrier height between the ErAs nanoparticles and the n-side of the tunnel junction. The n-side of the tunnel junction has a larger tunneling resistance than the p-side because the Schottky barrier height between the ErAs and GaAs conduction band is higher[16] ($\sim$0.9 eV) and also the doping on the n-side of the TJ is lower. It has been observed previously[17,18] in ErAs:InGaAs superlattices that the Fermi level moves closer to the conduction band edge, with decreasing nanoparticle size, leading to a lower n-Schottky barrier. This is consistent with the dependence of the n-Schottky barrier height of ScErAs films grown on vicinal GaAs surfaces.[16] Such a variation in the n-Schottky barrier height with nanoparticle size could also account for the observed trend in the tunnel junction resistance. To further investigate the effect of nanoparticle size on tunnel junction resistance, tunnel junctions were grown with a fixed ErAs deposition (2 ML) while the growth temperature was varied. Lower growth temperatures produce smaller nanoparticles while the number density of nanoparticles increases to conserve the total amount of ErAs in the layer. As seen in Fig. 4, the tunnel junction resistance increased with the growth temperature. Although this seems to agree with the general idea that tunneling into smaller particles is more favorable than tunneling into larger particles, local conductivity measurements could provide more direct evidence.

We have demonstrated ErAs nanoparticle-enhanced tunnel junction with extremely low tunnel junction resistance of $1.73\times10^{-4}\ \Omega\ \mathrm{cm}^2$, $\sim10\times$ lower than previously reported.[8] The variation in tunnel junction resistance with growth temperature and amount of ErAs deposited indicates a competition between surface coverage and ErAs nanoparticle morphology that warrants further investigation as it can be used to fine tune and further enhance the performance of these tunnel junctions.

This work was supported by the Army Research Office (Grant No. W911NF-07-1-0528), monitored by Dr. Mike Gerhold, and the Defense Advanced Research Projects Agency through a Young Faculty Award (HR0011-08-1-0061).

[1] H. Cotal, C. Fetzer, J. Boisvert, G. Kinsey, R. King, P. Hebert, H. Yoon, and N. Karam, Energy Environ. Sci. **2**, 174 (2009).
[2] A. R. Adams, M. Asada, Y. Suematsu, and S. Arai, Jpn. J. Appl. Phys. **19**, L621 (1980).
[3] J. J. Wierer, P. W. Evans, N. Holonyak, and D. A. Kellogg, Appl. Phys. Lett. **71**, 3468 (1997).
[4] R. R. King, C. M. Fetzer, P. C. Colter, K. M. Edmondson, J. H. Ermer, H. L. Cotal, Hojun Yoon, A. P. Stavrides, G. Kinsey, D. D. Krut, and N. H. Karam, Conference Record of the 29th IEEE Photovoltaic Specialists Conference, 2002 (unpublished), pp. 776–781.
[5] S. Ahmed, M. R. Melloch, E. S. Harmon, D. T. McInturff, and J. M. Woodall, Appl. Phys. Lett. **71**, 3667 (1997).
[6] M. Kamp, G. Morsch, J. Graber, and H. Luth, J. Appl. Phys. **76**, 1974 (1994).
[7] N. Suzuki, T. Anan, H. Hatakeyama, and M. Tsuji, Appl. Phys. Lett. **88**, 231103 (2006).
[8] P. Pohl, F. H. Renner, M. Eckardt, A. Schwanhäußer, A. Friedrich, Ö. Yüksekdag, S. Malzer, G. H. Döhler, P. Kiesel, D. Driscoll, M. Hanson, and A. C. Gossard, Appl. Phys. Lett. **83**, 4035 (2003).
[9] J. M. O. Zide, A. Kleiman-Shwarsctein, N. C. Strandwitz, J. D. Zimmerman, T. Steenblock-Smith, A. C. Gossard, A. Forman, A. Ivanovskaya, and G. D. Stucky, Appl. Phys. Lett. **88**, 162103 (2006).
[10] A. G. Petukhov, W. R. L. Lambrecht, and B. Segall, Phys. Rev. B **53**, 4324 (1996).
[11] C. Kadow, J. A. Johnson, K. Kolstad, J. P. Ibbetson, and A. C. Gossard, J. Vac. Sci. Technol. B **18**, 2197 (2000).
[12] B. D. Schultz and C. J. Palmstrøm, Phys. Rev. B **73**, 241407 (2006).
[13] T. Sands, C. J. Palmstrøm, J. P. Harbison, V. G. Keramidas, N. Tabatabaie, T. L. Cheeks, R. Ramesh, and Y. Silberberg, Mater. Sci. Rep. **5**, 99 (1990).
[14] M. W. Denhoff, J. Phys. D: Appl. Phys. **39**, 1761 (2006).
[15] H. Yamaguchi and Y. Horikoshi, Appl. Phys. Lett. **60**, 2341 (1992).
[16] C. J. Palmstrom, T. L. Cheeks, H. L. Gilchrist, J. G. Zhu, C. B. Carter, B. J. Wilkens, and R. Martin, in *38th National Symposium of the American Vacuum Society* (AVS, Seattle, 1992), pp. 1946–1953.
[17] D. C. Driscoll, M. Hanson, C. Kadow, and A. C. Gossard, J. Vac. Sci. Technol. B **19**, 1631 (2001).
[18] C. Kadow, J. A. Johnson, K. Kolstad, and A. C. Gossard, J. Vac. Sci. Technol. B **21**, 29 (2003).

Author complimentary copy. Redistribution subject to AIP license or copyright, see http://apl.aip.org/apl/copyright.jsp